1-8-2009

Rapid effects of 17beta-estradiol on TRPV5 epithelial Ca2+ channels in rat renal cells.

Mustapha Irnaten
Royal College of Surgeons in Ireland

Nicolas Blanchard-Gutton
Royal College of Surgeons in Ireland

Jeppe Praetorius
Univeristy of Aarhus, Denmark

Brian J. Harvey
Royal College of Surgeons in Ireland

Citation

Irnaten M, Blanchard-Gutton N, Praetorius J, Harvey BJ. Rapid effects of 17beta-estradiol on TRPV5 epithelial Ca2+ channels in rat renal cells. Steroids. 2009;74(8):642-9.

Rapid effects of 17β-estradiol on TRPV5 epithelial Ca^{2+} channels in rat renal cells

Mustapha Irnaten[1]*, Nicolas Blanchard-Gutton[1]*, Jeppe Praetorius[2], and Brian J. Harvey[1]

1. Molecular Medicine Laboratories, Royal College of Surgeons in Ireland, Beaumont Hospital, PO Box 9063, Dublin 9, Ireland

2. Institute of Anatomy & the Water and Salt Research Center, University of Aarhus

Wilhelm Meyers Alle, bld,. 1-234.DK-8000 Aarhus, Denmark

Running title: REGULATION OF A RENAL CA^{2+} CHANNEL BY 17β-ESTRADIOL

Correspondence: Dr. Mustapha Irnaten, Department of Molecular Medicine, RCSI Education & Research Centre, Beaumont Hospital, P.O. Box 9063, Dublin 9, Ireland.
Phone: (+353) 85 133 4932; E-mail: irnatenm@yahoo.fr

* These authors have contributed equally to this work.

Abstract

The renal distal tubules and collecting ducts play a key role in the control of electrolyte and fluid homeostasis. The discovery of highly calcium selective channels, Transient Receptor Potential Vanilloid 5 (TRPV5) of the TRP superfamily, has clarified the nature of the calcium entry channels. It has been proposed that this channel mediates the critical Ca^{2+} entry step in transcellular Ca^{2+} re-absorption in the kidney. The regulation of transmembrane Ca^{2+} flux through TRPV5 is of particular importance for whole body calcium homeostasis.

In this study, we provide evidence that the TRPV5 channel is present in rat cortical collecting duct ($RCCD_2$) cells at mRNA and protein levels. We demonstrate that 17β–estradiol (E_2) is involved in the regulation of Ca^{2+} influx in these cells via the epithelial Ca^{2+} channels TRPV5. By combining whole-cell patch-clamp and Ca^{2+}-imaging techniques, we have characterized the electrophysiological properties of the TRPV5 channel and showed that treatment with 20 to 50 nM E_2 rapidly (< 5 min) induced a transient increase in inward whole-cell currents and intracellular Ca^{2+} via TRPV5 channels. This rise was significantly prevented when cells were pre-treated with ruthenium red and completely abolished in cells treated with siRNA specifically targeting TRPV5.

These data demonstrate for the first time, a novel rapid modulation of endogenously expressed TRPV5 channels by E_2 in kidney cells. Furthermore, the results suggest calcitropic effects of E_2. The results are discussed in relation to present concepts of non-genomic actions of E_2 in Ca^{2+} homeostasis.

Key Words: estrogen; renal cortical collecting duct; epithelial calcium channel; TRPV5.

1. Introduction

Calcium metabolism is of crucial importance to many vital physiological functions and the maintenance of the body Ca^{2+} homeostasis is essential to life. The modulation of intracellular Ca^{2+} activity by Ca^{2+} influx is one of the most universal signal transduction pathways in all cell types, from sensory signal transduction, cell growth, cardiovascular functions to gene expression [1]. Extracellular fluid calcium levels are handled and regulated by calcitropic hormones at three potential sites including, the gastrointestinal tract, kidney and bone. It is well established that Ca^{2+} is reabsorbed in kidney by a transcellular pathway. Ca^{2+} enters the epithelial cell passively across the apical membrane *via* Ca^{2+}-selective channels down an electrochemical gradient, diffuses through the cytosol bound to intracellular proteins as calbindins and parvalbumin and actively extruded at the basolateral membrane through Ca^{2+} ATPase activity and Na/Ca exchange [2].

Hormones, which are classically involved in Ca^{2+} homeostasis, include 1,25-dihydroxyvitamin D_3, parathyroid hormone and calcitonin [3; 4]. The idea that estrogen plays a role in Ca^{2+} homeostasis has been also established [5]. The involvement of 17β-estradiol (E_2) in Ca^{2+} homeostasis is clearly illustrated by the role of the hormone in bone mineralization and the finding that E_2 deficiency in postmenopausal women results in bone loss arising from a negative Ca^{2+} balance [6; 7], which is associated with a rise in plasma and urinary Ca^{2+} [8]. However, studies have shown that the rise in urinary Ca^{2+} at menopause is not due to an increased filtered load, suggesting that E_2 also has a role in regulating renal Ca^{2+} handling [9]. Ca^{2+} supplementation can also reduce bone loss in these patients, suggesting an interaction between estrogen deficiency and Ca^{2+} balance [10]. However, the cellular mechanisms underlying E_2 regulation of Ca^{2+} reabsorption is still poorly understood in kidney.

A family of Ca^{2+}-permeable cation channels has been discovered in the early 1990's; the Transient Receptor Potential (TRP) channels [11]. TRPV5 is a member of the TRPV subfamily [12] which is implicated in apical calcium entry in epithelia [13], shows a constitutive activity, and functions as a facilitative transporter. Although our knowledge of TRPV5 channel physiology is still relatively limited, TRP mutations have already been described that lead to kidney diseases [14].

Because transcellular Ca^{2+} transport is fine-tuned to the body's specific requirements, regulation of the transmembrane Ca^{2+} flux through TRPV5 is of particular importance for whole body Ca^{2+} homeostasis and is tightly controlled by hormones [15].

It has been demonstrated that TRPV5 protein expression is highly modulated by E_2 in kidney [16]. In addition to genomic effects, it is well established that E_2 can also exert rapid non-genomic effects on intracellular Ca^{2+} in various cell types: including hepatocytes, osteoblasts, enterocytes/monocytes and in distal colon [17-21]. Furthermore, there is increasing evidence for rapid, non-genomic, effects of E_2 on epithelial ion transport [22-25]. In particular, in the kidney collecting duct M-1 cells, E_2 has been shown to modulate intracellular Ca^{2+} levels through a calcium entry pathway [26]. On the basis of others and our previous studies, we hypothesize that E_2 may have the ability to regulate renal Ca^{2+} re-absorption through rapid effects on TRPV5 channel activity.

Most electrophysiological studies to date on TRPV5 channels have been performed on over expressing channels in heterologous systems, CHO and HEK being the most commonly employed cell models. Our study is one of the few reports of hormonal modulation of endogenous TRPV5 channels.

1. Experimental

1.1 Cell Culture

$RCCD_2$ cell line used in this study was previously characterized by Prof N. Farman's group. Immortalized RCCD2 cells were obtained by infection of primary cultured CCD cells with the wild-type simian virus 40. It has been shown that this cell line has maintained many of the original properties of rat CCD from which they were derived [28]. $RCCD_2$ cells were cultured in 75 cm^2 flasks or 35 mm glass-bottom dishes that had been coated with rat type I collagen, as previously described [27, 28]. Cells were cultured in a medium that contained 1:1 Ham's F-12-DMEM with 14 mM $NaHCO_3$, 20 mM HEPES buffer (pH 7.4), 10 U/ml penicillin-streptomycin, 2 mM glutamine, 5 μg/ml insulin, 50 nM dexamethasone, 5 μg/ml transferrin, 30 nM sodium selenite, 10 nM triiodothyronine, 10 ng/ml EGF, and 2% FBS (Gibco, Paisley, UK). RCCD2 cells were

maintained in serum-free medium and in the absence of dexamethasone and EGF overnight before treatment with oestrogen.

2.2 RT-PCR analysis

Total mRNA was isolated using *TRI-REAGENT*® (Molecular Research Center, USA) according to the manufacture's directions. Total RNA was reverse-transcribed into cDNA using *ImProm-II™ Reverse Transcription System* (Promega, USA). Primers for TRPV5 (accession no. NM_019841) were designed using *GeneFisher*-software [29], and synthesized by *MWG* (Germany).

The primers used for amplification of TRPV5 were [Forward: ACCACTACAGGAAGC-GTA; Reverse: CCGTCAATGATGGTAAGGA]. PCR amplification was performed with initial heating for 2 min at 94 °C, followed by 35 cycles of 1 min denaturation at 94 °C, annealing for 1 min at 51.5 °C and extension for 2 min at 72 °C. BLASTN search was performed on primers to confirm that the sequences were not shared with other known genes. The PCR products were resolved using a 1 % Tris-Borate-EDTA (TBE) agarose gel and the bands were analyzed *via* Gene Tools software (Syngene, UK). cDNA bands corresponding to TRPV5 transcripts were extracted from the agarose gel, purified using Quiaquick kit (Quiagen, UK) and subsequently sequenced (MWG, Germany).

2.3 Western blot analysis

Western blotting experiments were carried out using standard technique with modifications [30]. Briefly, cells were gently washed twice with PBS and scraped into SDS sample buffer [62.5 mM Tris-HCl (pH 6.8 at 25 °C), 2 % w/v SDS, 10 % glycerol, protease inhibitors and 2 mM DTT]. Equal amounts of total protein were resolved on 8 % SDS-PAGE gels and transferred onto polyvinyl difluoride membranes using the semi-dry transfer technique. Membranes were blocked for 2 hr at room temperature in Tris Buffered Saline with Tween-20 (TBST) containing 5% non-fat dry milk and incubated for 1 hr at room temperature with rabbit-anti rat TRPV5 primary antibody diluted in blocking solution, (1/500 dilution), (ACC-035, Alomone labs). Membranes were washed 3x10 min in TBST and incubated for 1 hr with HRP-Rabbit secondary antibody (1/5000 dilution in TBST containing 5 % dried milk). After 3x10 min wash, immuno-reactive

proteins were detected using enhanced ECL plus chemiluminescent reagent (Amersham Biosciences, UK).

Anti-β-actin monoclonal antibody (1/4000 dilution; Sigma, Ireland) was used as a loading control. Rat kidney cortex whole lysate and Chinese Hamster Ovary (CHO) cells were used as positive and negative controls, respectively.

2.4 Immunofluorescence microscopy

Four male Wistar rats were anesthetized by isoflurane inhalation and kidneys were perfusion fixed with 3% formaldehyde in phosphate buffer, pH 7.4 through the abdominal aorta. The tissues were dehydrated in graded ethanol, incubated overnight in xylene, and embedded in paraffin wax. 2 μm thick sections were cut using a rotary microtome (Leica, Heidelberg, Germany). The sections were dewaxed with xylene and rehydrated with graded ethanol. Endogenous peroxidase was blocked by 0.5% H_2O_2 in absolute methanol for 10 min. The sections were boiled in 10 mM tris with 0.5 mM EGTA, pH 9, for 10 min. After cooling, the sections were washed with 50 mM NH_4Cl in PBS for 30 min followed by incubation with PBS blocking buffer containing 1% BSA, 0.2% gelatin, and 0.05% saponin. The sections were incubated overnight at 4ºC with primary antibodies diluted in PBS supplemented with 0.1% BSA and 0.3% Triton X-100. Upon wash in PBS supplemented with 0.1% BSA, 0.2% gelatin, and 0.05% saponin dual or triple color fluorescence labeling were performed. The sections were incubated with fluorophore conjugated secondary antibodies (see below) in PBS supplemented with BSA and Triton-X-100. After washing, sections were mounted with a cover slip in Glycergel Antifade Medium (Dako), and inspected on a Leica DMRS confocal microscope using an HCX PlApo 64x (1.32 NA) objective.

2.5 Antibodies

Primary antibodies were: mouse anti-calbindin D-28K (Research Diagnostics, Flanders, NJ) and rabbit anti-TRPV5 (ECAC1AP, alpha diagnostics). Fluorescent secondary antibodies were donkey anti-rabbit Alexa488 and donkey anti-mouse Alexa555 (Invitrogen/Molecular Probes, Eugene, OR). Topro3 was used as a nuclear marker (Invitrogen).

2.6 Electrophysiology

It was impossible to patch $RCCD_2$ cells after 48 hr plating as the cells are flattened and whole-cell access configuration is difficult to achieve (Basolateral membrane not accessible to the bath solution changes). We therefore detached subconfluent cells from 6 well plates using trypsin–EDTA. After centrifugation at 1100 rpm for 3 min cells were recovered in culture medium at room temperature.

Patch-clamp experiments were performed using the whole-cell patch-clamp configuration [31]. Isolated $RCCD_2$ cells were transferred into a 1ml superfusion chamber mounted on the stage of an inverted microscope (Nikon) and perfused with modified Krebs "bath" solution. Patch pipettes were prepared from capillary glass (GC150 F-10, Harvard Apparatus Ltd, UK) using a puller (DMZ-Universal Puller, Zeitz-Instruments, Germany) and had a resistance of 3 to 5 MΩ when filled with the pipette solution. The reference electrode was an Ag-AgCl wire in direct contact with the superfusion bath. The patch–clamp apparatus consisted of a CV-203BU head stage (Axon Instruments Inc., CA, USA) connected to an Axopatch 200B series amplifier (Axon). Seal resistance was typically in the 1-5 GΩ range. Recorded membrane whole-cell currents were amplified and digitized at 5 kHz and low pass-filtered at 1 kHz. Membrane voltage was clamped from –120 mV to +100 mV with steps of 20 mV. Average capacitance of the cell was approximately 14.5 ± 2.2 pF. Drug actions were measured only after steady-state conditions were reached.

2.7 Calcium-Imaging microscopy

Initially we used the same concentration of E_2 (20 nM) in calcium imaging and patch-clamp experiments, but E_2 did not show any significant effect on intracellular calcium in calcium imaging. This could be due to the fact that at this concentration (20 nM) the accessibility of E_2 is limited to the apical side of the cells. For Ca^{2+} measurements cells were not trypsinised and were plated in glass cover slips and the basolateral membranes of the cells are stuck to the glass cover slip limiting drug and bathing solution access. However, in patch-clamp experiments, trypsinisation of cells allows the access of E_2 to the whole-cell membrane.

$RCCD_2$ cells were loaded for 45 minutes with 5 μM FURA-2/AM. All experiments were performed in physiological solution (as above), at room temperature (20-22^oC). Ca^{2+} "free" experiments performed in Krebs solution where calcium is omitted as previously described by Nilius *et al.* [12]. Cells were mounted on an inverted epi-fluorescence microscope (Diaphot 200, Nikon, Japan) and illuminated with a Xenon lamp (Cairn, UK) filtered through alternating 340 and 380 nm interference filters. The resultant fluorescence was passed through a 400 nm dichroic mirror, filtered at 510 nm and then collected using an intensified CCD camera system (Hammatsu, Japan). Images were recorded for 30 min, digitised and analysed using Openlab2 (Improvision, UK). Drug actions were measured only after steady-state conditions were reached.

2.8 Solutions and chemicals

For both calcium imaging and whole-cell patch-clamp experiments, cells were superfused with a "Krebs" solution containing (in mM): 145 NaCl; 6 CsCl; 1 $MgCl_2$; 10 $CaCl_2$ 10 HEPES and 10 glucose, pH 7.4 with CsOH. Na^+-free conditions were obtained by using $NMDG^+$ instead of Na^+. When the extracellular $CaCl_2$ concentration was increased, extracellular NaCl was equimolarly decreased respectively to keep the osmolarity constant. In divalent-free (DVF) solutions, Ca^{2+} and Mg^{2+} were omitted from the bathing solution. The patch pipette solution contained in all experiments (in mM): 20 CsCl; 100 Cs-Aspartate; 1 $MgCl_2$; 10 BAPTA (1,2-bis(2-aminophenoxy)ethane-*N,N,N',N'*-tetra-acetic acid); Na_2ATP 4, 10 HEPES (pH 7.2). Chemicals were purchased from Sigma Chemical Co. (Ireland). In all experiments, stock solutions of E_2 were prepared in methanol. No effect of the methanol vehicle on TRPV5 currents was observed at the concentrations used to study E_2 effects.

2.9 Synthesis and Transfection of siRNA for TRPV5

SiRNA sequences targeting rat TRPV5 were designed and synthesized using the Silencer Pre-designed siRNA construction kit (Ambion Research Inc., UK). The three specific TRPV5 target sequences used here are listed in table one.

$RCCD_2$ cells were splited and re-suspended in an Opti-MEM® I reduced Serum Medium (GIBCO, UK) for 12 hr prior to transfection. Sub-confluent cells (~ 50 % confluence) were transfected, between passages 10 to 25.

For each transfection, oligomer-Lipofectamine™ 2000 complexes were prepared as follows: (i) siRNA oligomer 50 pmol was diluted in 100 µl Opti-MEM® (Resulting concentration of siRNA is 100 nM) and the solution was gently mixed. (ii) Separately, Lipofectamine™ 2000 (5 µl) was diluted in 100 µl of Opti-MEM®. The solution was gently mixed and incubated for 5 min at room temperature. (iii) The diluted oligomer and Lipofectamine 2000 were gently mixed and incubated for 30 min at room temperature. The siRNA and Lipofectamine 2000 complex was added to 1 ml Opti-MEM® per well. Six-well plates were incubated at 37°C for 6 hr. thereafter; the medium was changed to a full culture medium for 48 hr.

For functional studies and to monitor transfection efficiencies cells were transfected with a FAM tagged siRNA. Functional non-coding siRNA#1 (Ambion Research Inc.) was used as a control.

2.10 Data analysis

The densitometry of the TRPV5 bands were normalized to the loading control, β-actin. Densitometric analysis of the western blots were performed using GeneTools software (SYNGENE, Cambridge UK). All data are reported as mean ± S.E.M for a series of the indicated number of experiments. Patch-clamp data analysis was performed using the clampfit software of the p-clamp suite version 9.2 and Origin 7.5 (OriginLab Corp, MA, USA). Statistical analysis of the data was obtained using a paired t-test for analysis between two groups, a p value < 0.05 was considered significant. One-way ANOVA was used for multiple analyses of more than two groups.

3. Results

3.1 Expression and electophysiological properties of TRPV5 in $RCCD_2$ Cells

We explored the presence of TRPV5 channels in $RCCD_2$ cells by RT-PCR. Figure 1A shows a single band of about 550 bp corresponding to TRPV5 transcript in $RCCD_2$ cells.

Subsequent sequencing of the band confirmed that it corresponded to the cDNA sequence of TRPV5. To further confirm the expression of TRPV5 in $RCCD_2$ cells, Western blot analysis was performed and revealed a band with a molecular size of ~ 90 kDa, corresponding to TRPV5 protein (Figure 1B). Rat kidney cortex was included as a positive control for both RT-PCR and Western blot. CHO cells were included as negative control for Western immunoblotting. To evidence the presence of TRPV5 in cortical collecting ducts, immunolocalization experiments were performed. Immunofluorescence microscopy revealed that luminal anti-TRPV5 immunoreactivity extends from the calbindin-positive late distal convoluted tubules (DCT2) and connecting tubules (CNT) into a subset of cells of the initial cortical collecting ducts (iCCD, Figure 1C). These patterns were observed in all four rats tested. Thus, luminal anti-TRPV5 labelling was restricted to DCT2, CNT and iCCD. Anti-TRPV5 staining was not detected in any other renal structures.

Based on these results, we investigated the electrophysiological properties of TRPV5 in these cells. Figure 2A compares the whole-cell current bathed with either external solution containing 1, 10 and 100 mM Ca^{2+} or in divalent free (DVF) solution with Na^+ as the major charge carrier of the currents. Under DVF solution, cells generated large inward currents that are completely abolished by replacing extracellular NaCl with NMDG-Cl. Re-application of NaCl to the bathing solution re-established the inward currents. Figure 2B show the current-voltage (I-V) relationship in the presence of increasing $[Ca^{2+}]_e$ (in mM: 1.5, 10, 20 and 100). Extracellular Ca^{2+} induces inward current with amplitude that depends on the $[Ca^{2+}]_e$ indicating that it is carried by Ca^{2+}.

We examined the effects of various membrane holding potentials on whole-cell currents in $RCCD_2$ cells. Figure 3A shows typical whole-cell current traces recorded at -120 mV at different holding potentials of +20, -50, -80 and -110 mV as indicated in the graph. Whole-cell current measurements showed that current amplitudes increased in a voltage-dependent manner upon hyperpolarization (Figure 3B). At a holding potential of -110 mV, the current measured at -120 mV was larger than the currents recorded at the same voltage when initiated from more depolarised holding potentials (-1242 ± 117 pA at -110 mV; -997 ± 121 pA at -80 mV; -312 ± 89 pA, at -50 mV; -88 ± 71 pA at +20 mV, n = 7). In addition, I-V profiles characterized by inward rectification at negative membrane

potentials recorded in these cells resemble those of TRPV5 previously reported by Clapham *et al.* [32]. These results support the hypothesis that calcium influx may occur *via* TRPV5 in $RCCD_2$ cells.

A dose-response study of the rapid effects of E_2 on whole-cell Ca^{2+} currents was performed in $RCCD_2$ cells (Figure 4). Treatment with increasing concentration of E_2 (in nM; 1, 10, 20, and 50) stimulated inward whole-cell Ca^{2+} currents in a dose-dependent manner. Cells generated inward currents that amplitudes increases from -225 ± 87 pA at 1nM E_2 to -306 ± 108 pA at 10 nM E_2, - 844 ± 122 pA, at 20 nM E_2 and to - 788 ± 113 pA at 50 nM E_2, n = 9). The maximum peak current amplitude obtained was at 20 nM E_2 therefore, we used this concentration for subsequent studies in all patch clamp experiments.

3.2 Intracellular Ca^{2+} rise induced by E_2 is sensitive to ruthenium red in $RCCD_2$ cells

3.2.1 Calcium imaging

The effect of 20 nM E_2 on $[Ca^{2+}]_i$ was examined in $RCCD_2$ cells. As shown in Figure 5A, E_2 treatment modulates cytosolic Ca^{2+} levels. In 35 % (n = 108) of the cells examined, E_2 induced a rapid transient peak rise in $[Ca^{2+}]_i$. Vehicle controls (physiological solution alone or with $5x10^{-5}$ % methanol) had no effect on $[Ca^{2+}]_i$ (Figure 5A).

To test if the E_2-induced increase in $[Ca^{2+}]_i$ originated from an extracellular source, we monitored the effect of E_2 in $RCCD_2$ cells bathed with "low" (1.5 mM) extracellular Ca^{2+}) solution. Under these conditions, E_2 treatment did not alter $[Ca^{2+}]_i$, and subsequent thapsigargin treatment triggered a rise in intracellular Ca^{2+} indicating that the release of calcium ions from internal stores was still possible but was not activated by E_2. These data indicate that the rise in $(Ca^{2+})_i$ induced by E_2 is initiated by an influx of Ca^{2+} into the cell from the extracellular space and not by an initial release from intracellular stores.

To investigate the contribution of TRPV5 in the E_2-induced Ca^{2+} rise cells were pre-treated with ruthenium red, a well-known effective blocker of highly-Ca^{2+} selective channels [33]. Figure 5B shows that E_2 induced a rise in Ca^{2+} of 18.3 ± 1.6 % above basal (n = 38 cells) this rise was significantly reduced to 9.7 ± 0.6 % above basal (n = 25 cells, $p < 0.002$) when cells were pre-treated with ruthenium red (50 μM).

Interestingly, the number of cells responding to E_2 with a rise in Ca^{2+} was also significantly decreased when cells were pre-treated with ruthenium red (19% in ruthenium red + E_2 vesus 35% of cells responding in E_2 alone, n = 131).

Taken together, these data further strengthen the conclusion that E_2 stimulates calcium influx *via* TRPV5 in $RCCD_2$ cells.

3.2.2 Patch-clamp

$RCCD_2$ cells were stimulated with E_2 in the presence or absence of ruthenium red. Figure 6 illustrates representative whole-cell current traces in (a) control (untreated) and in E_2 (20 nM) treated cells in the absence (b) or presence (c) of ruthenium red (50 μM). Addition of ruthenium red to the bath induces substantial decrease in current amplitudes. Figure 6 d shows I-V relationship measurements demonstrating that E_2 application stimulated a mean maximal increase in inward whole-cell currents. E_2 increased whole-cell current amplitudes from basal values in control (untreated) cells of -222 ± 47 pA to -734 ± 68 pA at a Vp = -120 mV (n = 10, $p < 0.01$). Adding ruthenium red significantly reduces the E_2-activated mean maximal increase in whole-cell currents from -734 ± 68 pA to -255 ± 57 pA at a Vp = -120 mV (n = 7, $p < 0.02$), corresponding to a reduction in current of approximately 65%.

The whole-cell conductance (Gc) calculated over the Vp range –120 to –60 mV was increased to 403 ± 23 pS (n = 10, $p < 0.01$) with E_2 treatment compared to control untreated cells (111 ± 5 pS). Exposure of cells to ruthenium red (50 μM) reduced the E_2 - induced Gc to 119 ± 12 pS (n = 7, $p < 0.02$), which was not significantly different from the Gc recorded in control (untreated) cells, (111 ± 5 pS, n = 7, $p>0.05$). These data reinforce the conclusion of the contribution of TRPV5 channels in response to E_2 induced whole-cell inward Ca^{2+} currents in $RCCD_2$ cells.

3.3 E_2-induced calcium entry channels activation is suppressed by siRNA targeting TRPV5 in $RCCD_2$ cells

As ruthenium red has been only reported as an effective but not specific inhibitor of TRPV5 channel [33], siRNA has been employed to specifically suppress TRPV5 expression and activity. Three different siRNAs (siRNA#1, siRNA#2 and siRNA#3)

targeting different sequences of TRPV5 were tested in $RCCD_2$ cells (Table 1). Figures 7A and B illustrate the expression of TRPV5 protein in control siRNA (Functional non-coding siRNA #1, Ambion Research Inc., UK) and three TRPV5-siRNAs transfected $RCCD_2$ cells. Western blot analysis revealed no significant decrease in TRPV5 expression following transfection of individual siRNA (Figure 7A, B; Lane 2-4). However, combination of co-transfections is more efficient. The most efficient silencing expression of TRPV5 was the co-transfection with siRNA#2 and #3 (Lane 7). Therefore, co-transfection of $RCCD_2$ cells with siRNA#2 and#3 has been used for functional studies and the control functional non-coding siRNA#1 has been used as control-siRNA. The possibility that the calcium influx is mediated by TRPV6 has been tested and no significant knockdown expression of TRPV6 was obtained when cells were transfected or co-transfected with different siRNA targeting TRPV5 (Figure 7A). Western blot in Figure 7A TPRV6 expression seems to be downregulated by some siRNAs, particularly siRNA 2 and 3. This is a representative Western blot, on average of three different experiments, no statistically significant difference has been found.

Figure 8 shows (A) a typical I-V relationship experiment and (B) averaged data of whole-cell Ca^{2+} currents entering through TRPV5 obtained at the first voltage step of -120 mV. The results showed that E_2 induced inward whole-cell currents rise in cells transfected with control functional non-coding siRNA, but E_2 failed in cells co-transfected with siRNA#2/3, corresponding to E_2 control of -1089 ± 92 pA (at Vp = -120 mV), (n = 12, p <0.005) compared to E_2 responses in siRNA#2/3 cells of -141 ± 44 pA (at Vp = -120 mV), (n = 6, p <0.005). Taken together, these results demonstrate that co-transfection with siRNA#2/3 substantially decreased TRPV5 protein expression level leading to the inhibition of TRPV5 activity and E_2 activation of $[Ca^{2+}]_i$ rise involving TRPV5 channels.

4. Discussion

This study provides, for the first time, evidence of a rapid stimulatory effect of 17β-estradiol on $[Ca^{2+}]_i$ involving TRPV5.

Using RT-PCR and Western blot analysis we have demonstrated that TRPV5 is present at both mRNA and protein expression levels in $RCCD_2$ cells. We have also provided

evidence for expression of TRPV5 in native iCCD in addition to the DCT2 and CNT localization. Using the patch-clamp technique, we studied the electrophysiological properties of Ca^{2+}-dependent channels in $RCCD_2$ cells. In the presence of monovalent cations and Ca^{2+} these channels initially display decrease of currents as extracellular Ca^{2+} levels are reduced, but at very low extracellular Ca^{2+} levels, currents then increase beyond the amplitude observed in the presence of high extracellular Ca^{2+} levels, due to the increasing permeability to monovalent cations including Na^+, loss of selectivity in the absence of divalent cations. This behaviour is thought to be related to the affinity difference between monovalent and divalent cations in the channel pore. These Na^+/Ca^+ selectivity features are in agreement with those reported previously by Nilius B et al., 2001. Whole-cell current was minimal over a ± 100mV range under 1.5 mM Ca^{2+} conditions and was significantly activated by increasing $[Ca^{2+}]_e$. The Ca^{2+}-dependent whole-cell current could also be activated at any given extracellular calcium concentration by membrane hyperpolarization. The $[Ca^{2+}]_e$ and voltage dependence characteristics are known features of TRPV5 channels and, taken together with the RT-PCR and Western blotting data, indicate the functional expression of TRPV5 channels in $RCCD_2$ cells.

The E_2-induced whole-cell and $[Ca^{2+}]_i$ were increased when cells were exposed to increasing $[Ca^{2+}]$ in the bath solution, indicating that Ca^{2+} influx is initiated from the extracellular compartment and involves Ca^{2+} entry into the cell. Patch-clamp measurements performed under similar conditions demonstrated that the whole-cell conductance has been substantially decreased and remained unaffected by E_2 treatment when Ca^{2+} was removed from the extracellular bathing solution. Ruthenium red is known to be the most effective blocker of TRPV5 (IC_{50}= 111nM), [33].

In RCCD2 cells, the maximum inhibitory effect of ruthenium red (RR) was obtained only at 50 μM, 1-10 μM RR have been tested and no significantly inhibitory effect on the E_2 induced currents was observed (data not shown). Pre-treatment of cells with 50 μM ruthenium red in the bathing solution significantly reduced the number of cells responding with a rise in $[Ca^{2+}]_i$ after E_2 exposure. Moreover, patch-clamp analysis showed a decrease in whole-cell conductance by 70% when the cells were pre-treated

with ruthenium red before E_2 stimulation. These results implicate Ca^{2+} entry *via* possibly TRPV5 during E_2 response.

SiRNA knockdown was employed as an alternative approach to specifically suppress TRPV5 channel expression and activity. To assess the importance of TRPV5 expression in $RCCD_2$ cells, and its contribution to E_2 induced rise in $[Ca^{2+}]_i$, specific siRNA was transfected into $RCCD_2$ cells. Since different siRNAs targeting the same gene are often differentially effective in silencing the expression of their target, three different siRNAs (siRNA#1, siRNA#2 and siRNA#3) directed against different target sequences in rat TRPV5 were transfected into $RCCD_2$ cells (Table 1). Combined co-transfection with siRNA#2 and siRNA#3 showed substantial silencing of TRPV5 protein expression level in $RCCD_2$ cells. To associate the expression silencing to functional silencing, whole-cell current measurements were performed in TRPV5 siRNA transfected cells compared to control functional non-coding siRNA treated cells. The siRNA knockdown experiments clearly provide the evidence of the contribution of TRPV5 in E_2-induced Ca^{2+} influx in $RCCD_2$ cells.

As the latency of onset of steroid hormone genomic responses is approximately 30 min, our results represent a rapid (within 3 to 6 minutes) non-genomic response to E_2. The physiological role for non-genomic action of 17β–estradiol in renal cortical duct cells may serve to enhance the retention and re-absorption of Ca^{2+}. Taken together, the results of our studies indicate that 17β-estradiol induces a rapid intracellular calcium response *via* Ca^{2+} entry through the epithelial Ca^{2+} channels TRPV5 in $RCCD_2$ cells. The signaling mechanisms and receptor(s) involved in E_2 modulation of TRPV5 channels and their role in transepithelial Ca^{2+} transport remain to be identified.

To date TRPV5 has not been localized to CCD while TRPV6 has. Thus we showed that TRPV6 is expressed in these cells. Further, the close homology between these channels may falsely identify one as the other despite several approaches. Functionally, it will be hard to discriminate between both channels. To this end proof that the siRNA and antibody is specific for TRPV5 and not TRPV6 has been preformed. To discriminate between TRPV5 and TRPV6, Western blot experiments demonstrated that si-RNA-TRPV5 knock-down does not affect the expression of TRPV6 (see Fig. 7A). In addition, based on knock-down functional experiments (i.e. in both patch-clamp or Ca^{2+} imaging

experiments we haven't seen any significant $[Ca^{2+}]_i$ increase after E_2 stimulation in TRPV5-siRNA transfected cells), we concluded that TRPV5 play a key role in this Ca^{2+} response and we considered that TRPV5 was the major Ca^{2+} channel involved in response to E2 stimulation in RCCD2 cells.

Functional regulatory mechanism of TRPV channels by estrogen in renal collecting duct cells is of great importance for the better understanding of transepithelial reabsorption of calcium and, as a consequence, may reveal novel pharmacological and therapeutic targets for the treatment of several disorders of calcium metabolism such as idiopathic hypercalciuria, stone disease and postmenopausal osteoporosis.

5. Acnowledgments

We thank Dr N. Farman for providing the $RCCD_2$ cell line. This research was supported by the Higher Education Authority (HEA), Ireland, Programme for Human Genomics PRTLI Cycle 3 grant, and by a Wellcome Trust Programme Grant (060809/Z/00/Z).

6. References

[1] M.J. Berridge, P. Lipp, M.D. Bootman, The versatility and universality of calcium signalling, *Nat Rev Mol Cell Biol*, 1 (2000), pp. 11-21.

[2] F. Bronner, Renal calcium transport: mechanisms and regulation--an overview, *Am J Physiol*, 257 (1989), pp. 707-711.

[3] A.H. Jr. Tashjian, Homeostasis of plasma calcium: effects of actinomycin D, parathyroidectomy and thyrocalcitonin, *Endocrinology* 77 (1965), pp. 375-381.

[4] A.W. Norman, H.L. Henry, H.H. Malluche, 24R,25-Dihydroxyvitamin D_3 and 1 alpha,25-dihydroxyvitamin D_3 are both indispensable for calcium and phosphorus homeostasis, *Life Sci* 27 (1980), pp. 229-237.

[5] R.L. Prince, Counterpoint: estrogen effects on calcitropic hormones and calcium homeostasis, *Endocr Rev* 15 (1994), pp. 301-309.

[6] M.M. Young, C. Jasani, D.A. Smith, B.E. Nordin, Some effects of ethinyl oestradiol on calcium and phosphorus metabolism in osteoporosis, *Clin Sci* 34 (1968), pp. 411-417.

[7] M.M. Young, B.E. Nordin, The effect of the natural and artificial menopause on bone density and fracture, *Proc R Soc Med* 62 (1969), pp. 242.

[8] B.E. Nordin, A. Horsman, D.H. Marshall, M. Simpson, G.M. Waterhouse, Calcium requirement and calcium therapy, *Clin Orthop Relat Res* 140 (1979), pp. 216-239.

[9] S. Adami, D. Gatti, F. Bertoldo, M. Rossini, A. Fratta-Pasini, N. Zamberlan *et al*., The effects of menopause and estrogen replacement therapy on the renal handling of calcium, *Osteoporos Int* 2 (1992), pp. 180-185.

[10] R.L. Prince, M. Smith, I.M. Dick, R.I. Price, P.G. Webb, N.K. Henderson *et al*., Prevention of postmenopausal osteoporosis. A comparative study of exercise, calcium supplementation, and hormone-replacement therapy, *N Engl J Med* 325 (1991), pp. 1189-1195.

[11] C. Montell and G.M. Rubin, Molecular characterization of the Drosophila trp locus: a putative integral membrane protein required for phototransduction, *Neuron* 2 (1989), pp. 1313-1323.

[12] J.G. Hoenharderop, A.W. van Der Kemp, A. Hartog, S.F. van de Graaf, C.H. van Os, P.H. Willems *et al*., Molecular identification of the apical Ca^{2+} channel in 1,25-dihydroxyvitamin D_3-responsive epithelia, *J Biol Chem* 274 (1999), pp. 8375-8378.

[13] B. Nilius, R. Vennekens, J. Prenen, J.G. Hoenderop, G. Droogmans, R.J. Bindels, The single pore residue Asp542 determines Ca^{2+} permeation and Mg^{2+} block of the epithelial Ca^{2+} channel, *J Biol Chem* 276 (2001), pp. 1020-1025.

[14] C. Montell, Physiology, phylogeny, and functions of the TRP superfamily of cation channels, *Sci STKE* 90 (2001), RE1.

[15] M.J. Berridge, Elementary and global aspects of calcium signalling, *J Physiol* 499 (1997), pp. 291-306.

[16] M. van Abel, J.G. Hoenderop, A.W. van der Kemp, J.P. van Leeuwen, R.J. Bindels, Regulation of the epithelial Ca^{2+} channels in small intestine as studied by quantitative mRNA detection, *Am J Physiol Gastrointest Liver Physiol* 285 (2003), pp. 78-85.

[17] A. Sanchez-Bueno, M.J. Sancho, P.H. Cobbold, Progesterone and oestradiol increase cytosolic Ca^{2+} in single rat hepatocytes, *Biochem J* 280 (1991), pp. 273-276.

[18] M. Lieberherr, B. Grosse, M. Kachkache, S. Balsan, Cell signaling and estrogens in female rat osteoblasts: a possible involvement of unconventional nonnuclear receptors, *J Bone Miner Res* 8 (1993), pp. 1365-1376.

[19] G. Picotto, V. Massheimer, R. Boland, Acute stimulation of intestinal cell calcium influx induced by 17 beta-estradiol *via* the cAMP messenger system, *Mol Cell Endocrinol* 119 (1996), pp. 129-134.

[20] C.M. Doolan, B.J. Harvey, Modulation of cytosolic protein kinase C and calcium ion activity by steroid hormones in rat distal colon, *J Biol Chem* 271 (1996), pp. 8763-8767.

[21] G.B. Stefano, V. Prevot, J.C. Beauvillain, C. Fimiani, I. Welters, P. Cadet *et al*., Estradiol coupling to human monocyte nitric oxide release is dependent on intracellular calcium transients: evidence for an estrogen surface receptor, *J Immunol* 163 (1999), pp. 3758-3763.

[22] B. MacNamara, D.C. Winter, J. Cuffe, G. O'Sullivan, B.J. Harvey, Mechanism of oestrogen-induced salt and water retention, *Surg Forum* 81 (1995), pp. 560-562.

[23] B. MacNamara, D.C. Winter, J. Cuffe, G. O'Sullivan, J. Geibel, B.J. Harvey, Real time imaging of the rapid nongenomic oestrogen effects on cellular ion transport, *Surg Forum* 83 (1997), pp. 522-524.

[24] S.B. Condliffe, C.M. Doolan, B.J. Harvey, 17b-Oestradiol acutely regulates Cl^- secretion in rat distal colonic epithelium, *J Physiol* 530 (2001), pp. 47-54.

[25] B.J. Harvey, R. Alzamora, V. Healy, C. Renard, C.M. Doolan, Rapid responses to steroid hormones: from frog skin to human colon. A homage to Hans Ussing, *Biochim Biophys Acta* 1566 (2002), pp. 116-128.

[26] B.J. Harvey, M. Higgins, Nongenomic effects of aldosterone on Ca^{2+} in M-1 cortical

collecting duct cells, *Kidney Int* 57 (2000), pp. 1395-1403.

[27] M. Blot-Chabaud, M. Laplace, F. Cluzeaud, C. Capurro, R. Cassingéna, A. Vandewalle *et al*., Characteristics of a rat cortical collecting duct cell line that maintains high transepithelial resistance, *Kidney Int* 50 (1996), pp. 367-376.

[28] S. Djelidi, A. Beggah, N. Courtois-Coutry, M. Jay, F. Cluzeau, S. Viengchareun *et al*., Basolateral translocation by vasopressin of the aldosterone-induced pool of latent Na-K-ATPases is accompanied by a_1-subunit dephosphorylation: study in a new aldosterone-sensitive rat cortical collecting duct cell line, *J Am Soc Nephrol* 12 (2001), pp. 1805-1818.

[29] R. Giegerich, F. Meyer, C. Schleiermacher, GeneFisher-Software Support for the Detection of Postulated Genes, *Proc Int Conf Intell Syst Mol Biol* 4 (1996), pp. 68-77.

[30] W.N.Burnette, "Western blotting": electrophoretic transfer of proteins from sodium dodecyl sulfate--polyacrylamide gels to unmodified nitrocellulose and radiographic detection with antibody and radioiodinated protein A, *Anal Biochem* 112 (1981), pp. 195-203.

[31] O.P. Hamill, A. Marty, E. Neher, B. Sakmann, F.J. Sigworth, Improved patch-clamp techniques for high-resolution current recording from cells and cell-free membrane patches, *Pflügers Archiv* 391 (1981), pp. 85-100.

[32] E. David Clapham. Sorting out MIC, TRP, and CRAC Ion Channels. *J Gen Physiol* 120: (2002), pp. 217-220.

[33] B. Nilius, J. Prenen, R. Vennekens, J.G. Hoenderop, R.J. Bindels, G. Droogmans, Pharmacological modulation of monovalent cation currents through the epithelial Ca^{2+} channel ECaC1, *Br J Pharmacol* 134 (2001), pp. 453-462.

Figure legends

Figure 1 *Expression of TRPV5 in $RCCD_2$ cells.* A) Agarose gel electrophoresis of mRNA products obtained by the RT-PCR method for amplifying base pair sequences for TRPV5. PCR product sizes were determined by comparing to DNA ladder (lane 1). The ~550 bp band represents TRPV5 (lane 2). No bands were obtained in negative controls with no mRNA template or reverse transcriptase (lane 3 and 4). Expression of TRPV5 mRNA in native tissue kidney cortex (lower panel) was included as a positive control. B) Western blot analysis of extracts from $RCCD_2$ cell lysates (Lane 2), rat kidney cortex (lane 1, positive control) and CHO cell lysates (lane 3, negative control). Blots were probed with Anti-TRPV5 antibody (Upper blot). Bands of ~ 90 kDa corresponding to the expected size of TRPV5 protein were detected in $RCCD_2$ cells and rat kidney cortex tissue but not in CHO cells. As a loading control, blots were stripped and reprobed with an anti-β-actin antibody (Lower blot). Bands corresponding to TRPV5 and β-actin are indicated by arrows and the corresponding molecular weight (kDa), respectively. The data are representative of 3 experiments. C) Immunohistochemical analysis of TRPV5 and calbindin D-28K in rat isolated CCD sections. Rat Kidney sections were incubated for overnight at 4 ºC with the corresponding primary antibodies mouse anti-calbindin-D28K (dilution: 1:40 000) and guinea rabit anti-TRPV5 (dilution 1:100). To visualize the proteins corresponding secondary Alexa 488/555 (dilution 1:1000) conjugated antibodies were used. Tropro3 (dilution 1: 1000) was used as a nuclear marker.

Figure 2 *Whole-cell currents are $[Ca^{2+}]_e$ dependent in $RCCD_2$ cells*. Whole-cell recordings were elicited from +20 mV holding potential in 20 mV steps from -120 mV to +100 mV. The patch pipette was filled with a standard cesium-aspartate solution supplemented with 10 mM of BAPTA. Cells were first perfused with DVF solution then with increasing of extracellular Ca^{2+} concentrations. A) Whole-cell currents were recorded in DVF conditions. The presence of Na^+ as the major charge carrier in the external solution resulted in large inward current amplitudes which were completely abolished when Na^+ was replaced by $NMDG^+$. Addition of 1, 10 and 100 mM of Ca^{2+} in monovalent free external solution induced an inward transient current that amplitude

depends on the $[Ca^{2+}]_e$. B) Current/voltage relationships recorded by measuring the amplitude of currents at: 1.5 mM Ca^{2+} (▼), 10 mM Ca^{2+} (■), 20 mM Ca^{2+} (●) and 100 mM Ca^{2+} (▲). Data are mean ± SEM, n = 7 cells obtained from 7 separate experiments.

Figure 3 *Whole-cell currents are voltage-dependent in $RCCD_2$ cells.* Cells were incubated in Krebs solution containing 10 mM Ca^{2+} in the perfusion medium and 10 mM BAPTA in the pipette solution. From a holding potential of +20 mV the membrane potential was changed to -50 mV, -80 mV and -110 mV. Currents were measured at the first voltage step of -120 mV. **(A)** Original typical whole-cell currents traces recorded at different holding potentials as indicated in the graph. **(B)** Averaged data representing currents recorded from 7 cells at different holding potentials at the first step of –120 mV. Data represent the mean ± S.E.M of 7 cells.

Figure 4 *Effect of E_2 on whole-cell currents in RCCD2 cells*. Whole-cell recordings were elicited from +20 mV holding potential in 20 mV steps from -120 mV to +100 mV in $RCCD_2$ cells. Cells were allowed to stabilize and dialyze for at about 5 minutes before exposure to E_2. Treatment of cells with increasing concentrations of E_2 (in nM: 1, 10, 20, 50) induced a dose-dependent current amplitudes increases**.** The maximum peak increase was obtained at 20 nM E_2. The results shown are tracings of representative cells with similar results observed in separate experiments from 9 cells. Arrow indicates time of addition of E_2.

Figure 5 *17β-estradiol induces increase in $[Ca^{2+}]_i$ in $RCCD_2$ cells.* **A)** Addition of E_2 (50 nM) induced a rapid increase in $[Ca^{2+}]_i$ (■). E_2-induced $[Ca^{2+}]_i$ increase were typically rapid in onset and transient and returned to basal levels within 1-2 min**.** No increase in $[Ca^{2+}]_i$ levels were observed in response to vehicle (5.10^{-5} % methanol), (●), or physiological solution alone (▲). The X-axis represents time after the drug addition (the arrow represents time of E_2 addition). All measurements have been normalized with the base line emission wavelength ratio being fixed at 1. As a positive control to store filling, thapsigargin (1 µM) was added to the bathing solution at the end of each experiment. **B)** *E_2-induced Ca^{2+} entry is sensitive to ruthenium red.* 50 nM E_2 induced a significant

increase over control $[Ca^{2+}]_i$ (normalized increase above basal = 118 ± 2 ; n = 38 vs control 100, n_t = 38). Pre-incubation with the potent TRPV5 blocker, ruthenium red (50 μM), significantly inhibited the E_2-induced increases in $[Ca^{2+}]_i$ to 110 ± 1 (n = 25). Values are presented as means ± S.E.M. (*denotes significant differences: *** $p <$ 0.001).

Figure 6 *E_2-induced inward Ca^{2+} currents are sensitive to ruthenium red.* Cells were stimulated with 20nM E_2, either in the presence or absence 50 μM of ruthenium red (RuR), or "low" (1.5 mM) extracellular Ca^{2+} conditions. The pipette solution was supplemented with 10 mM BAPTA. **(a)** Typical whole-cell current traces recorded in control (untreated) cells. **(b)** Typical whole-cell current traces recorded in E_2 treated cells (20 nM E_2). **(c)** Typical whole-cell current traces recorded showed that the increase of Ca^{2+} currents induced by E_2 treatment was prevented when cells were pretreated for 15 min with 50 μM RuR. **(d)** Current / voltage relationships of TRPV5 channels: 20 nM E_2 in "low" Ca^{2+} conditions (■); Krebs supplemented with 10 mM Ca^{2+}, 20 nM E_2 + 50 μM RuR (▲); 20 nM E_2 alone (●). Data represent the mean ± S.E.M of 7 cells ($p < 0.02$).

Figure 7 *SiRNA knockdown of rat TRPV5 protein expression in $RCCD_2$ cells.* **A)** Western blot experiments performed with total protein prepared from $RCCD_2$ epithelial cells. *Lane 1:* non-coding siRNA transfected cells (control); *lane 2, 3 and 4:* Transfected cells with siRNA#1; #2 *and* #3, respectively. *Lane 5, 6, 7 and 8:* Combined co-transfected cells with siRNA#1 & #2; siRNA#1 & #3; siRNA#2 & #3; and siRNA#1, #2 & #3, respectively. **B)** Immuno-blot analysis showed that cells co-transfected with siRNA#2 *#3* are the most efficient for silencing TRPV5 protein expression relative to their controls. Functional non-coding control #1 (Ambion, LTD, UK) has been used as siRNA control. TRPV6 has been used as a control to examine the specificity of TRPV5 knockdown expression. Note that no significant knockdown expression of TRPV6 in all $RCCD_2$ cells transfected with different siRNAs targeting TRPV5. β-actin has been used as loading control. Data are representative of three similar experiments.

Figure 8 *Rapid effect of E_2 on Ca^{2+} currents in siRNA-TRPV5 transfected cells.* Patch clamp experiments were performed in cells either transfected with control siRNA or co-transfected with siRNA#2/3. Cells were treated with E_2 (20 nM) in the presence of 10 mM Ca^{2+} in the bath solution. A) Representative Current/voltage relationship experiment performed in cells transfected with functional non-coding siRNA (n = 8) and cells co-transfected with siRNA#2/3 (n = 8), B) Normalized data of E_2 induced TRPV5 currents recorded at the first voltage step of -120 mV from cells transfected with control siRNA and siRNA#2/#3. Data represent the mean ± S.E.M. (*** Indicates significant differences between control and transfected cells, $p < 0.02$).

Table 1: Target sequences of rat TRPV5 siRNA

Figure 1

Click here to download high resolution image

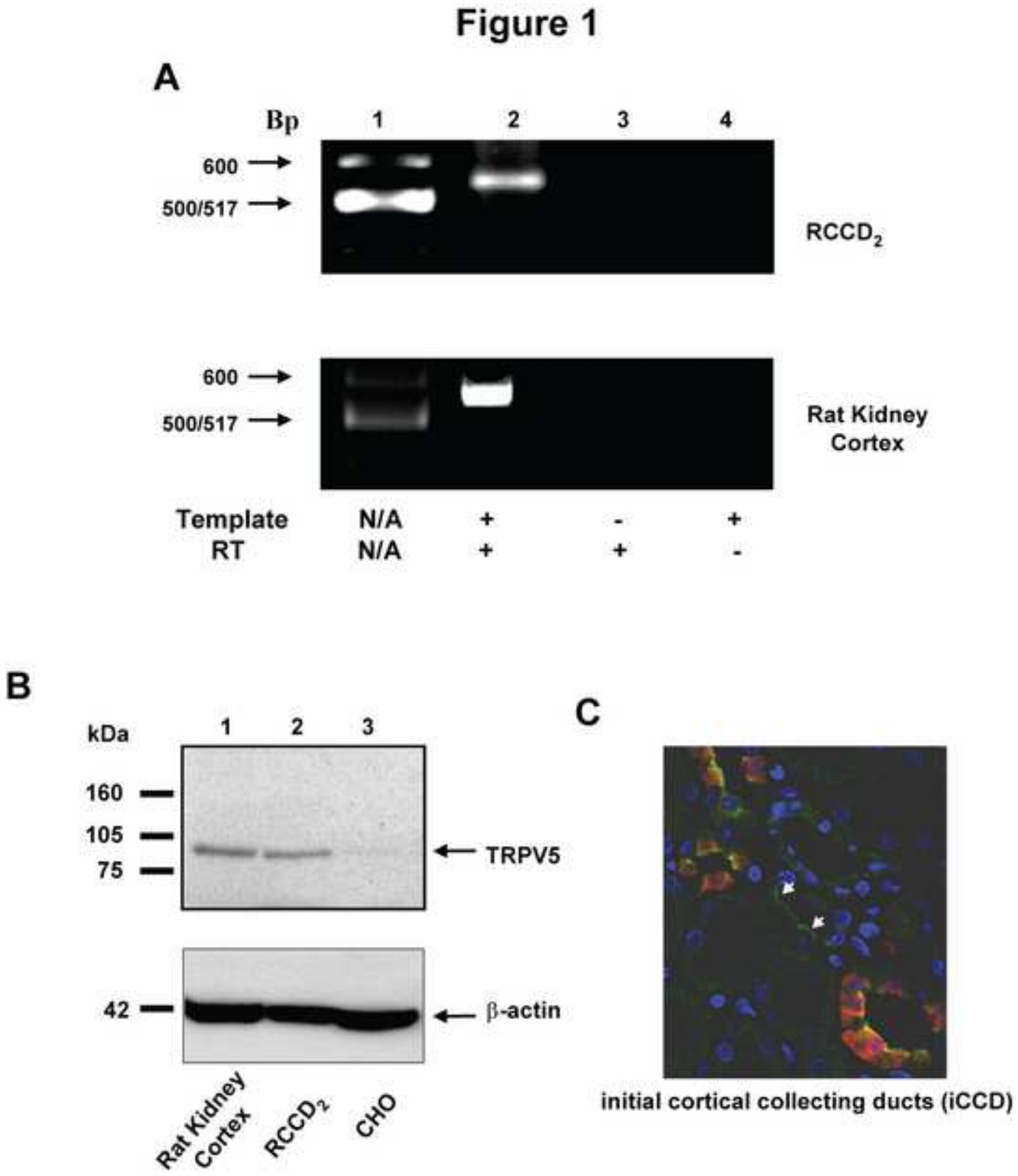

Figure 2
Click here to download high resolution image

Figure 2

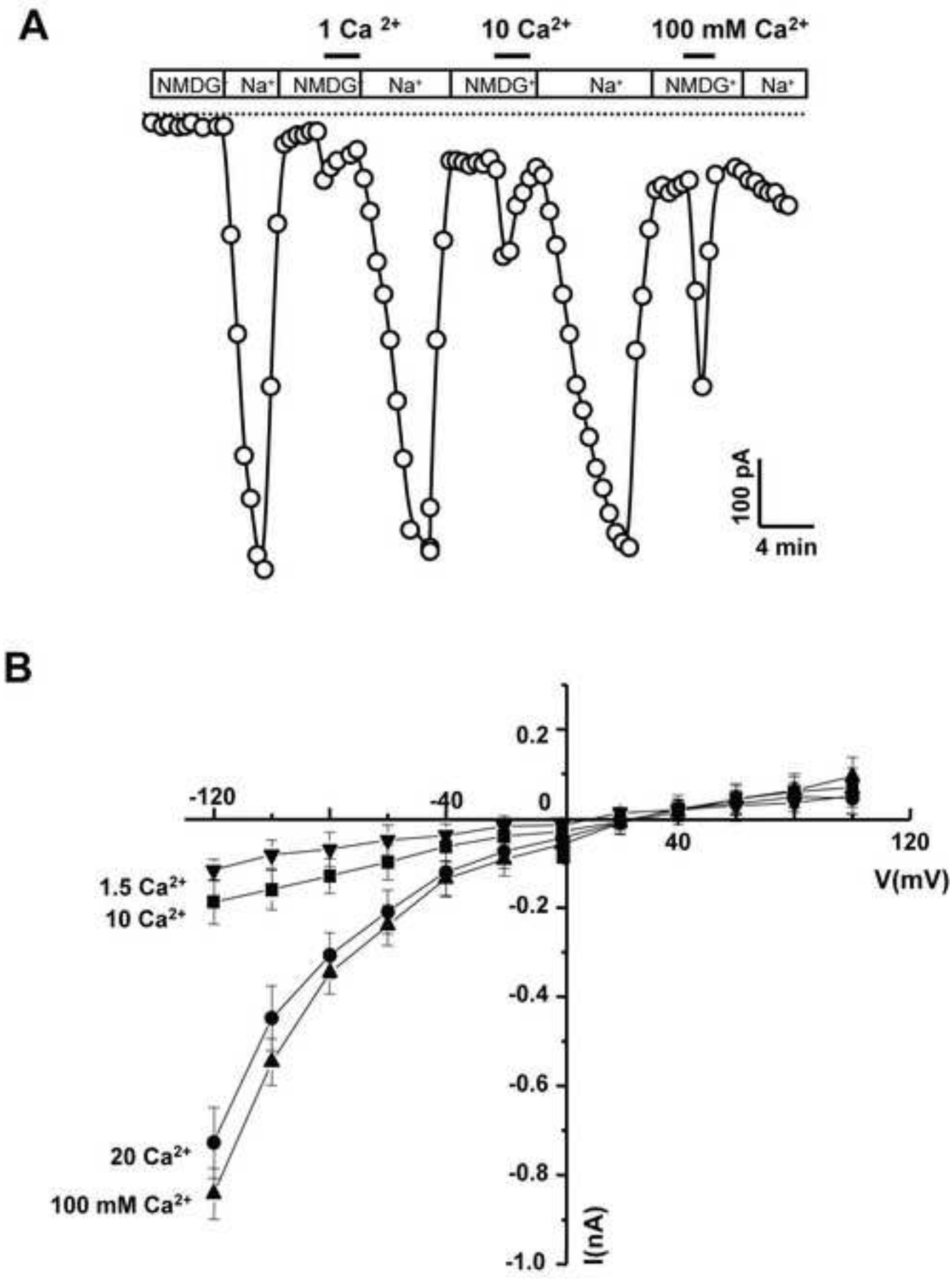

Figure 3
Click here to download high resolution image

Figure 3

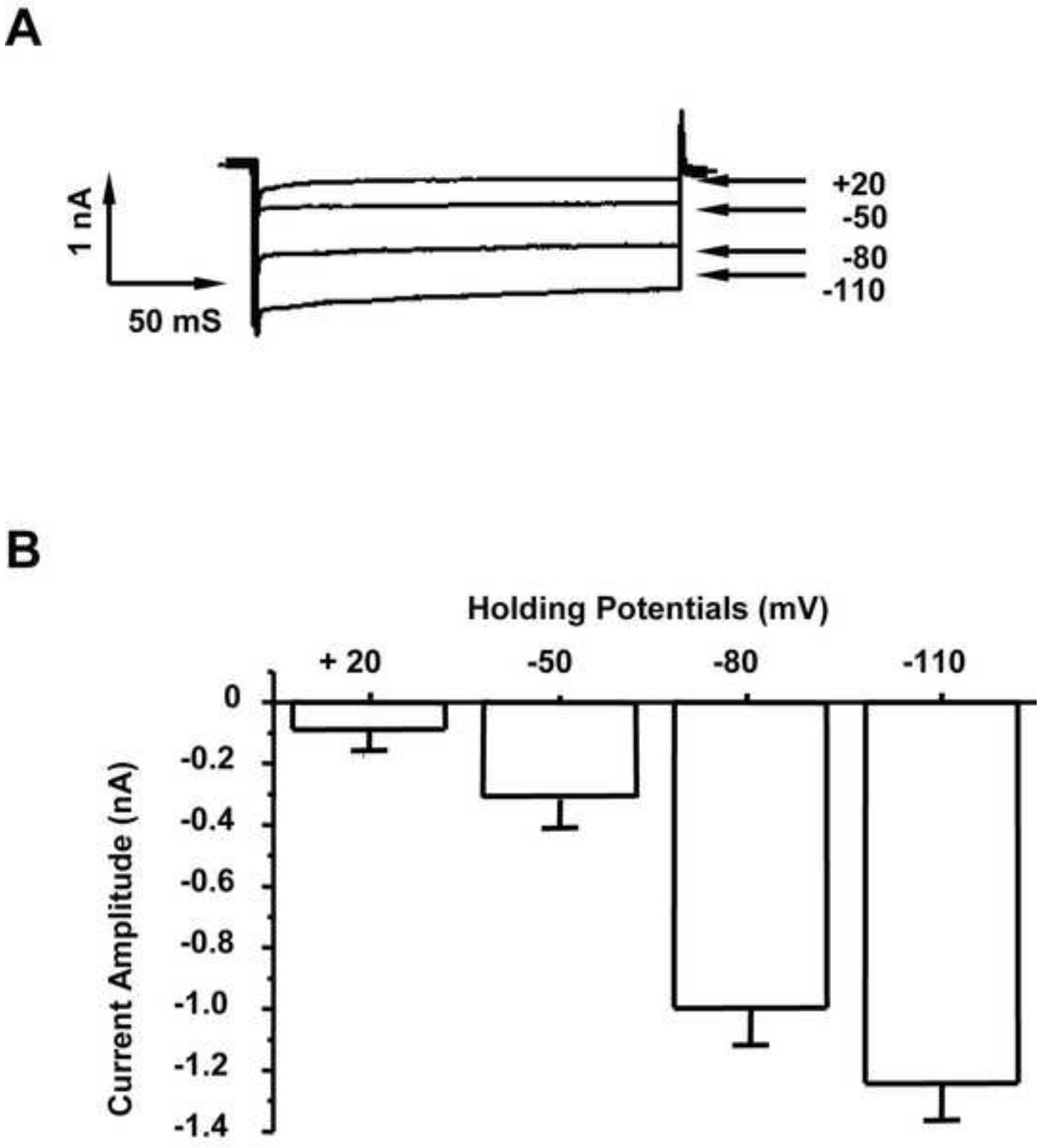

Figure 4

Click here to download high resolution image

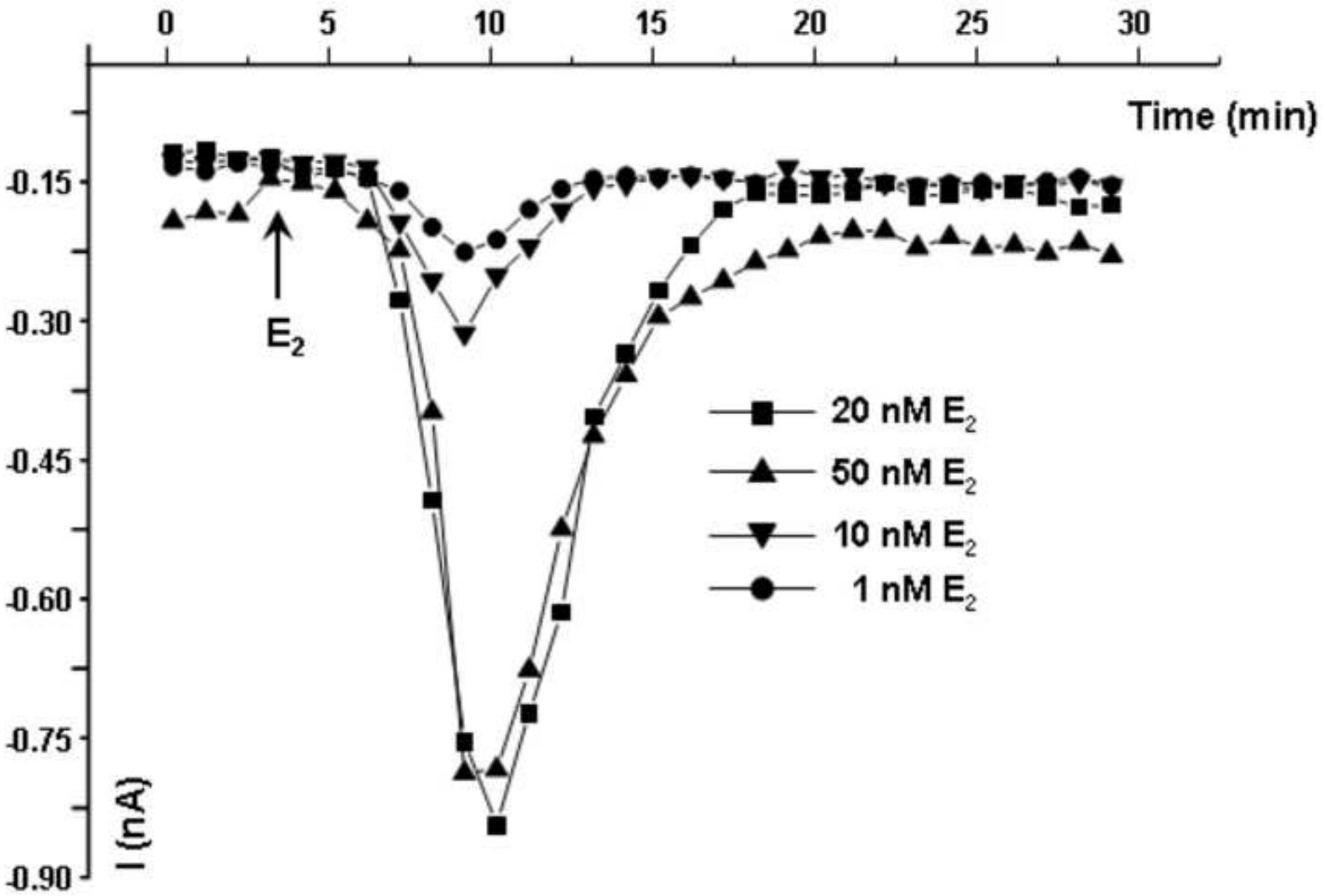

Figure 5

Click here to download high resolution image

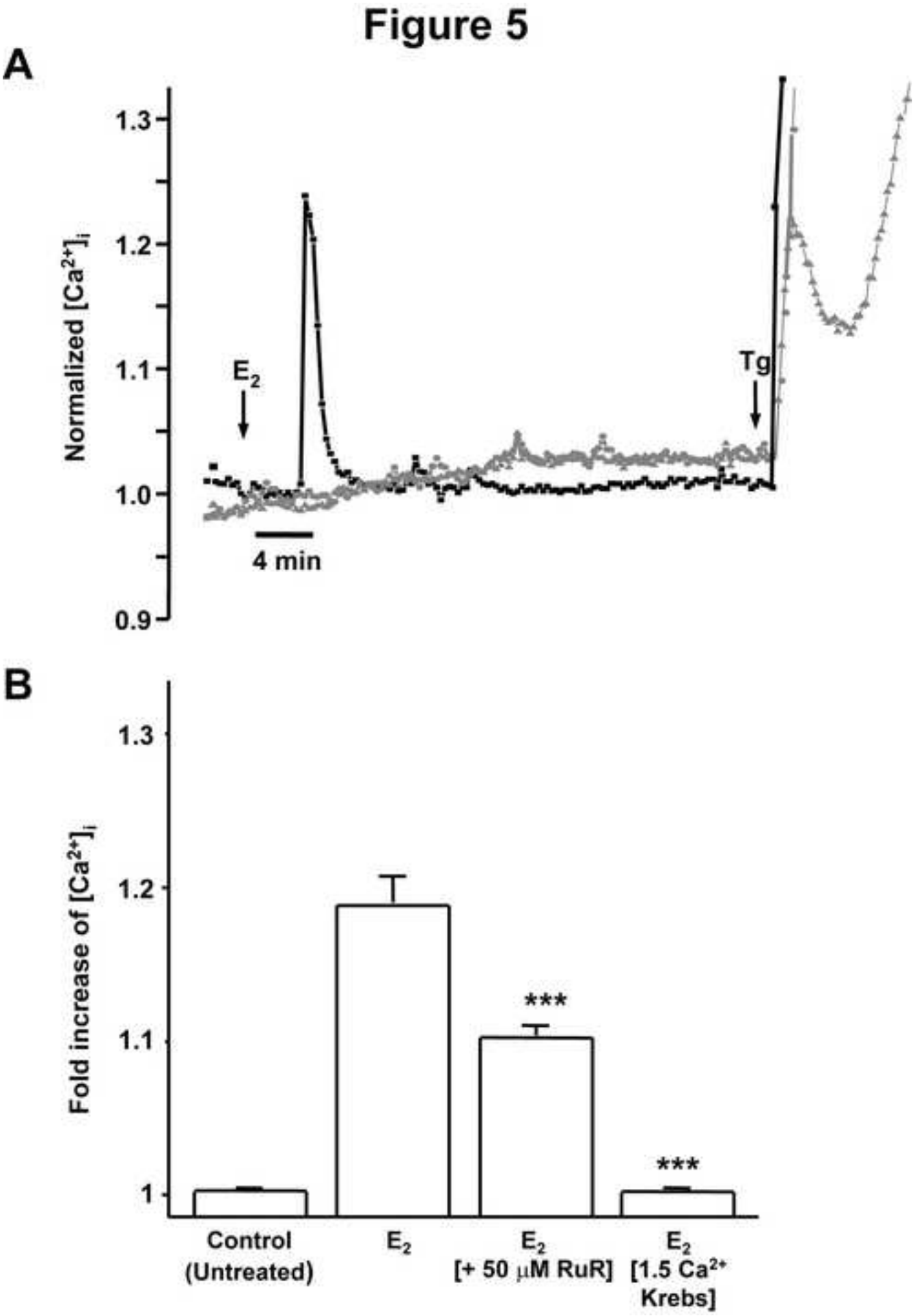

Figure 6

Click here to download high resolution image

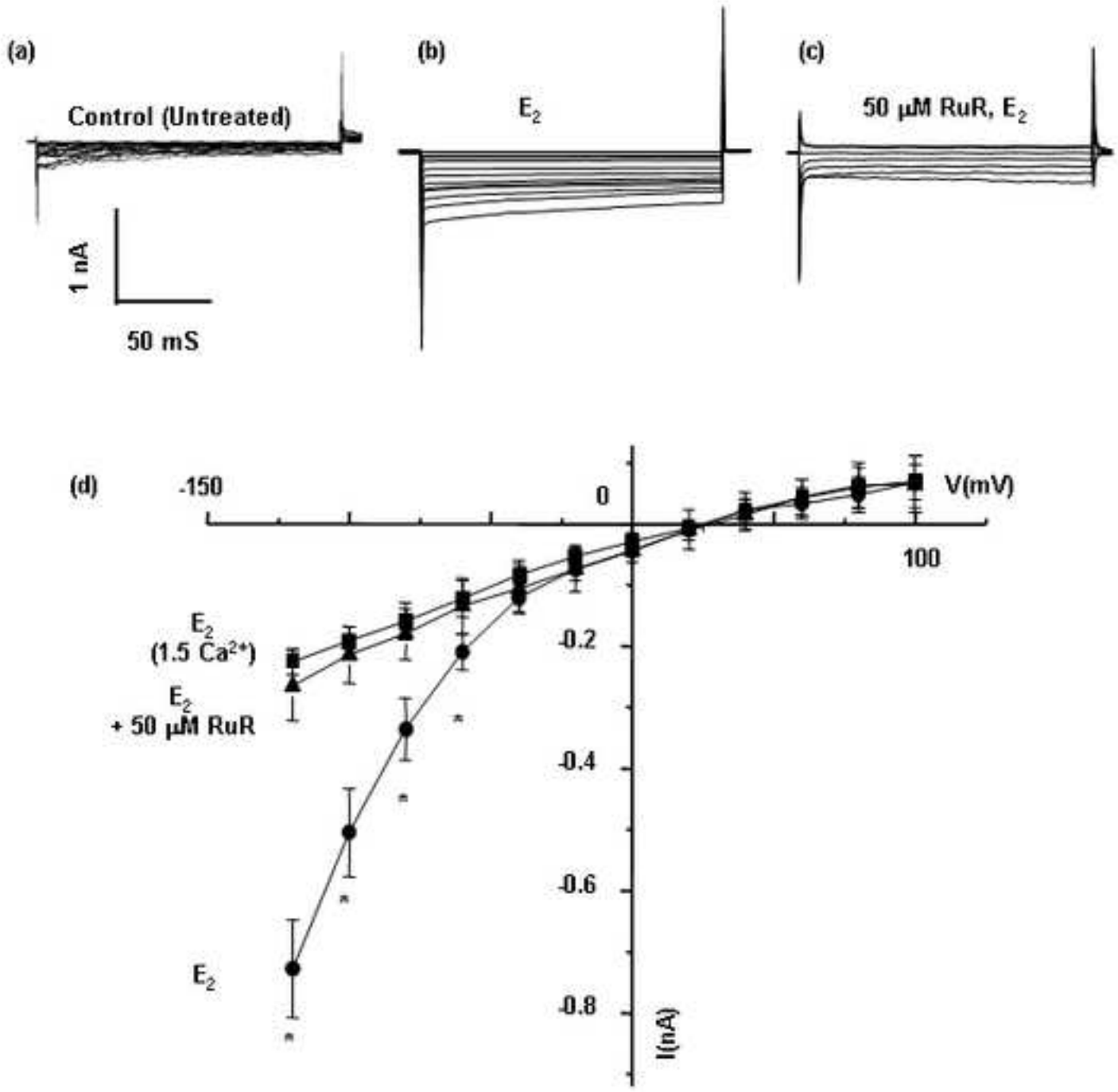

Figure 7

Click here to download high resolution image

Figure 7

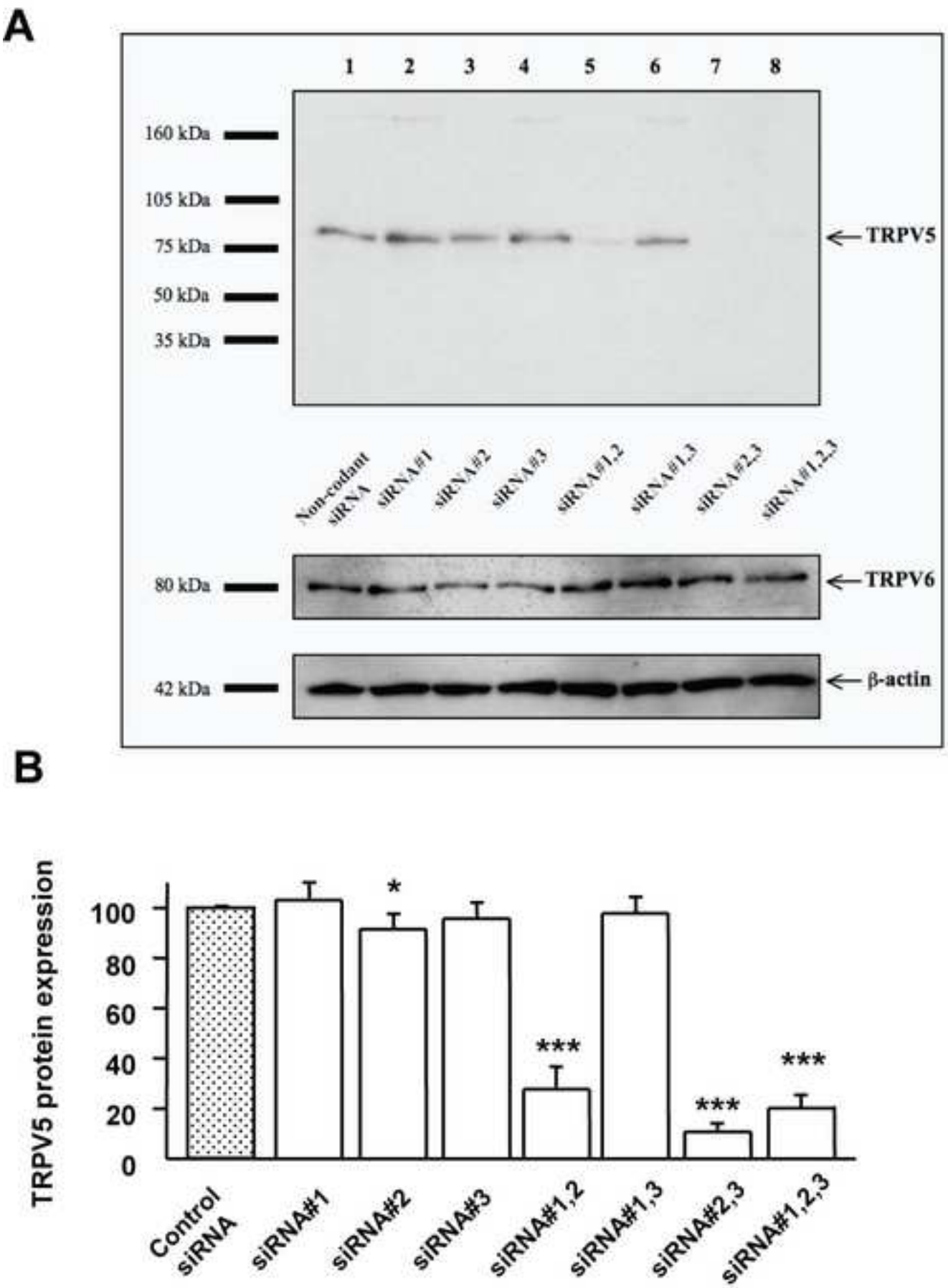

Figure 8

Click here to download high resolution image

Figure 8

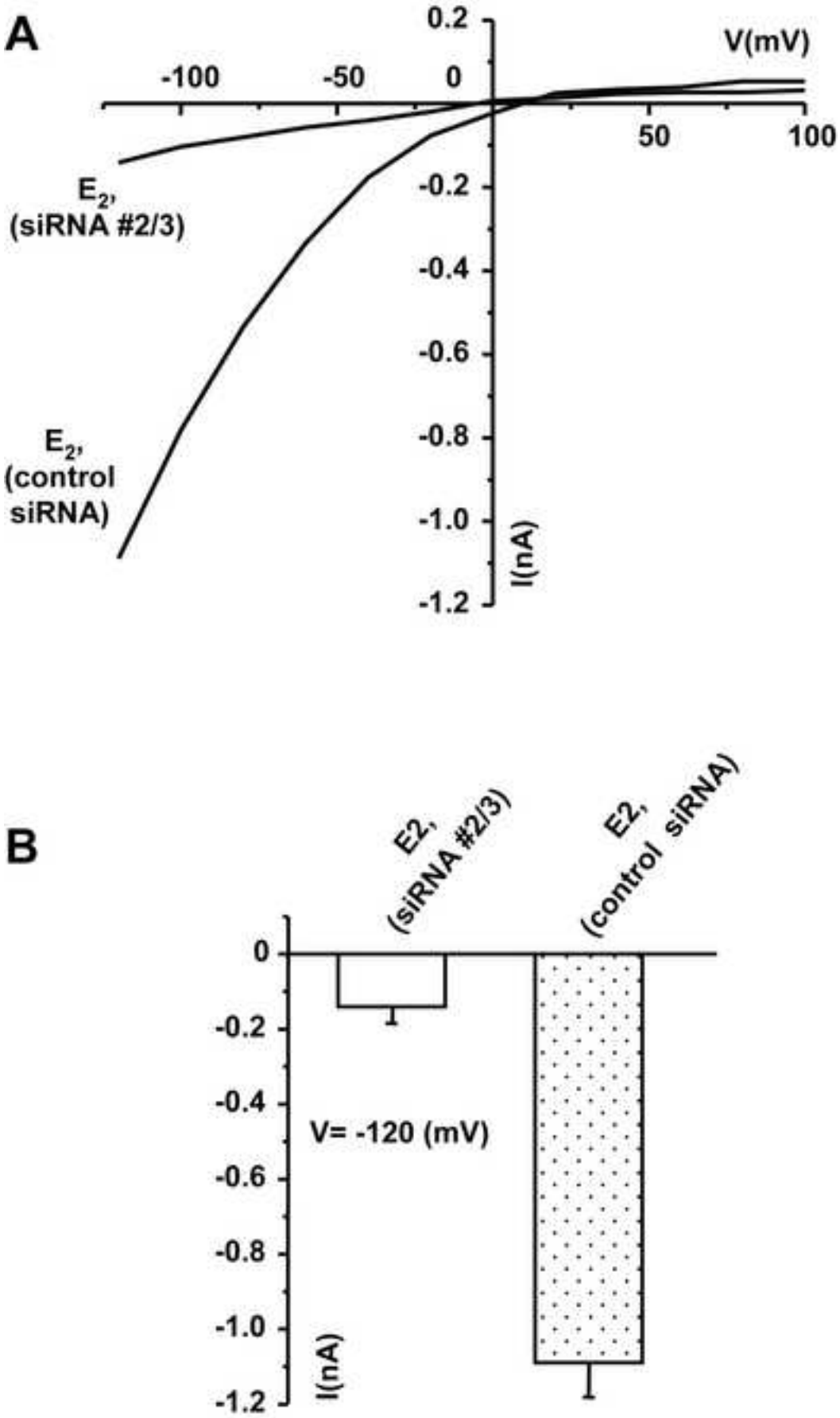

Table 1

Table 1

Target sequences of rat TRPV5 siRNA

siRNA	Target Sequences	Position in gene sequence	GC Content %
siRNA#1 sense	GCAUGUGGAUCAGCUUCAUtt	240-261	43
antisense	AUGAAGCUGAUCCACAUGCtg		48
siRNA#2 sense	GCUUCAUAUGCUACAGCAGtt	252-273	43
antisense	CUGCUGUAGCAUAUGAAGCtg		48
siRNA#3 sense	CGUAUAAUGUGGAAAGAACtt	2664-2685	33
antisense	GUUCUUUCCACAUUAUACGtt		33